Enhancing Load Frequency Control in Interconnected Power Systems with Zone-Specific Fuzzy Controllers

Shahrzad Jahangiri and Dr Karl O. Jones
School of Engineering
Liverpool John Moores University
Liverpool, United Kingdom, L3 3AF

shahrzadjahangiri.elec@gmail.com
K.O.Jones@ljmu.ac.uk

ABSTRACT

This work focuses on load frequency control in interconnected power systems, a critical aspect of modern power grid operations. However, sudden load disturbances and generator outages can lead to transient oscillations between control areas, posing challenges to frequency control. The aim of the work was to investigate and enhance load frequency control behaviour, considering dynamic load changes and uncertainties. Fuzzy Logic Controllers optimized with Particle Swarm Optimization were applied to improve control robustness. The Particle Swarm Optimisation algorithm was used to tune the scaling factors and parameters of the fuzzy controllers to optimize their performance. The methods were tested on a standard four-area interconnected power system model equipped with load frequency control blocks, reheaters, governors, rate constraints, and thermal components. Different disturbance scenarios including parameter fluctuations and load changes were evaluated. The Fuzzy Logic Controllers demonstrate resilient response across scenarios without needing extensive tuning. Particle Swarm Optimization improves robustness through systematic exploration for constraint-based nonlinear optimization. Tuning fuzzy controllers with bio-inspired algorithms enhances efficiency in addressing complex grid conditions. The results provide insights into designing more secure and resilient grid controls, contributing to power system stability research.

KEYWORDS: *Load Frequency Control, Interconnected Power Systems, Fuzzy Logic Controllers, Particle Swarm Optimization, Robust Control.*

1 INTRODUCTION

Electric power systems face increasing challenges owing to renewable integration, interconnection expansion, and deregulation (Haroun and Li, 2019), making frequency stability and power transmission reliability during disturbances more difficult. Load frequency control (LFC) is crucial for regulating frequency deviations and tie-line power flows across interconnected control areas (Sahu *et al.*, 2014; Panda *et al.*, 2009), but traditional strategies have limitations in responding to significant transients (Haroun and Li, 2017).

This work explores an adaptive intelligent optimization approach for LFC in multi-area power systems, focusing on bio-inspired algorithms such as Particle Swarm Optimization (PSO) (Pandey *et al.*, 2017), Genetic Algorithms (Saadat, 1999), and Ant Colony Optimization (Dhillon *et al.*, 2015; Sahu *et al.*, 2015; Dhillon *et al.*, 2016). A comprehensive evaluation and comparison of these techniques' optimization capabilities for LFC controller design was conducted. Fuzzy Logic Controllers (FLC) optimized adaptively (Abdel-Magidand Dawoud, 1995; Monfared *et al.*, 2015) are developed to enhance control robustness.

Testing was performed on a standard four-area thermal system equipped with LFC blocks, as shown in Figure 1 (Dong *et al.*, 2015), closely replicating real-world conditions. Simulations under various disturbance scenarios provide insights to advance grid control development, contributing to power system stability research.

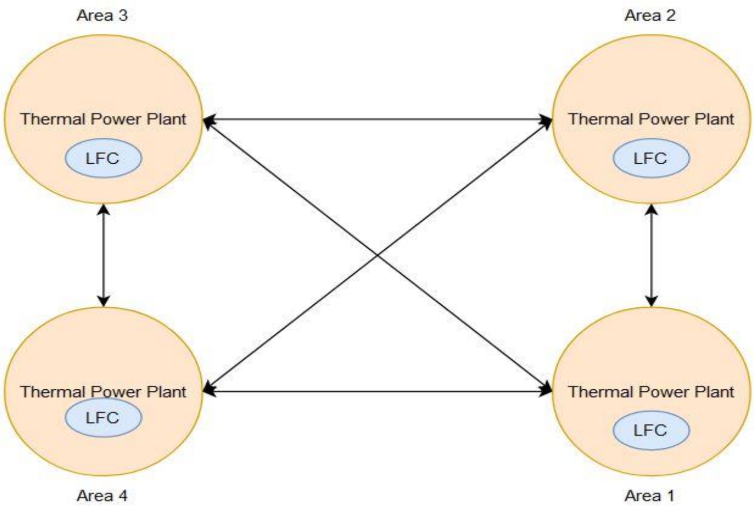

Figure 1 Interlinked four area power grids.

2 LITERATURE REVIEW

2.1 Limitations of Existing Load Frequency Control Approaches

The classic PID controller is widely used in industrial applications, but it faces challenges handling complex grid dynamics (Delassi *et al.*, 2018). The PID controller fixed parameters offer limited adaptability to changing conditions and nonlinearities (Panda *et al.*, 2009). Fuzzy controllers are a potential solution, although traditional PID tuning shows promise (Haroun and Li, 2017). Robust and adaptive control techniques address uncertainties and variations (Wenhui *et al.*, 2014; El-Bahay *et al.*, 2022; *Li et al.*, 2017). However, emerging Artificial Intelligence (AI) methods require further assessment (Vasant *et al.*, 2011).

2.2 Intelligent Algorithms and Optimization Techniques

Notable intelligent approaches include model predictive control (Vrabie *et al.*, 2009), fuzzy logic (Tripathy et al., 1982) and neural networks tuned via bio-inspired optimizations (Vasant *et al.*, 2011; Abdelaziz *et al.*, 2016), improving transient response over classical methods. Key bio-inspired optimizations algorithms include Particle Swarm Optimization (PSO) (Sahu *et al.*, 2015; Kennedy and Eberhart, 1995), Genetic Algorithms (GA) (Abdel-Magidand Dawoud, 1995; Monfared *et al.*, 2015), and Ant Colony Optimization (ACO) (Dhillon *et al.*, 2016; Afzalan and Jurabian, 2014). PSO offers faster convergence and consistency in finding optimal solutions for controller tuning (Vrabie *et al.*, 2009; Singh *et al.*, 2013). Further, GA and ACO also enhance adaptive PID and fuzzy designs (Sadaqati *et al.*, 2016).

2.3 Comparing Optimization Methods for Load Frequency Control

Comprehensive comparisons of PSO, GA, and ACO considering their distinct search mechanisms are lacking but are crucial to selecting the most effective technique (Afzalan and Jurabian, 2014). This work addresses this gap through multi-area power system studies assessing their optimization performance for load frequency control improvements (Shayeghi and Shayanfar, 2006).

3 PROPOSED RESEARCH METHODOLOGY

3.1 Fuzzy Logic Controller Optimization

Fuzzy logic controllers (FLCs) are integrated to enhance system control by handling uncertainty. An additional input signal u_e is introduced as in (1) to enable adaptive PID tuning (Zhang *et al.*, 2015). The FLC output $\bar{u}$ scales the PID gains through factors α and β as in (2). This structure optimizes the fuzzy PID (FLiPID) controller using the Particle Swarm Optimisation algorithm.

$$u_i = \frac{1}{\alpha}\left(-F + \dot{y}^* + K_p(ACE_i) + K_i \int (ACE_i)dt + K_d \frac{d(ACE_i)}{dt}\right) + u_e \quad (1)$$

Here, ū is the output of the FLC, scaled by factors α and β, enabling adaptive tuning of the PID gains.

$$u_e = \alpha\bar{u} + \beta \int \bar{u}dt \quad (2)$$

3.2 Performance Objective and Optimization

The integral of squared error (ISE) between frequency and tie-line power deviations as in (3) defines the objective function (Meena and Kumar, 2016). PSO iteratively minimizes this error under constraints (4) to determine optimal control parameters.

$$J = ISE = \int_0^{T_{sim}} \left(\Delta F_i^2 + \Delta F_{tie.ij}^2\right) dt \quad (3)$$

$$\begin{gathered} K_{pmin} \le K_p \le K_{pmax}, K_{imin} \le K_i \le K_{imax}, K_{dmin} \le K_d \le K_{dmax} \\ K_{1min} \le K_1 \le K_{1max}, K_{2min} \le K_2 \le K_{2max} \\ \alpha_{min} \le \alpha \le \alpha_{max}, \beta_{min} \le \beta \le \beta_{max} \end{gathered} \quad (4)$$

3.3 PSO Comparison with ACO and GA

PSO was compared to both ACO (Dhillon *et al.*, 2016) and GA (Abdel-Magidand Dawoud, 1995). Convergence performance towards the ISE objective was evaluated across these population-based methods. Key differences in their stochastic search mechanisms impact optimization outcomes in load frequency control.

4 SIMULATION RESULTS

4.1 Introduction

This section presents simulation results of optimized fuzzy PID controllers using PSO, ACO, and GA. MATLAB was employed for implementation, and controller performance is evaluated under varied power system conditions to reduce oscillations. Comparisons are made among optimization techniques using the Integral of Squared Error (ISE) chart as the objective function, offering insights into their effectiveness for tuning fuzzy PID controllers in dynamic power systems.

4.2 Simulation on a Four-Area Network

The optimization algorithm is applied to a four-area network, where parameters including K_i, K_d, K_p, α, β, K_1, and K_2 are optimized. The system diagram, depicted in Figure 1, illustrates the four-zone configuration comprising GDB, GRC constraints, thermal, and boiler systems. The system parameters used were adopted from Çam and Kocaarslan (2005), and are presented in Table 1. The simulations incorporated a 1% load disturbance within the connected multi-area power system.

Table 1. System parameter values.

Parameter	Value	Parameter	Value
Rating	2000 (MW)	T_{ij}	0.08674 (p.u.MW)
$P_{tie,\,ij}$	200 (MW)		
T_{pi}	20 (s)	**Boiler (gas or oil fired) data**	
K_{pi}	120 (Hz/p.uMW)	K_1	0.85
T_{ti}	0.3 (s)	K_2	0.095
T_{gi}	0.08 (s)	K_3	0.92
B_i	0.425 (p.u.MW/Hz)	C_B	200 (s)
R_i	2.4 (Hz/p.u.MW)	T_D	0 (s)
K_{ri}	0.5	T_F	10 (s)
T_{ri}	10 (s)	K_{1B}	0.03
ΔP_{L1}	0.01 (p.u.MW)	T_{1B}	26
a_{ij}	1.0 (p.u.)	T_{RB}	69 (s)

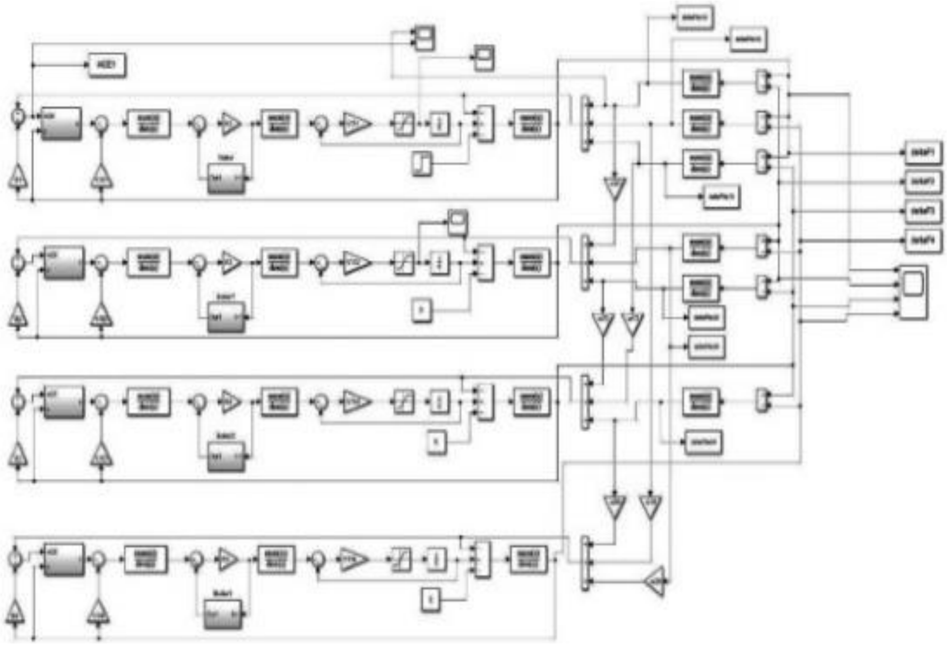

Figure 2 Block diagram model of a four-zone system

4.3 FLiPID Controller Optimization

Utilizing the PSO algorithm, the controller parameters of the FLiPID were optimized. The optimal controller parameters for four regions with uniform value are presented in Table 2.

Table 2. Optimise control parameters for four regions with identical values

Controller parameter	K_i	K_d	K_p	K_2	K_1	α	β
values	0.5000	0.4568	2.5385	4.4719	7.5587	0.0067	0.0133

Table 3 details the optimized FLiPID controller parameters for the four zones with distinct objective function values.

Table 3. Optimal FLiPID controller parameters for four zones with different objective function values

Controller Parameter	K_i	K_d	K_p	K_2	K_1	α	β
Different parameters Area 1	0. 3352	0.3525	2.4557	4.9748	5.2782	-0.0157	0.0056
Different parameters Area 2	0. 2528	0.4158	4.4717	4.8611	5.5586	-0.0169	0.0154
Different parameters Area 3	0.3074	0.3127	2.7067	5.9625	4.3739	-0.0088	0.0096
Different parameters Area 4	0.3024	0.4618	2.8850	4.0463	6.0695	-0.0196	0.0254

4.4 Simulation Results

The performance evaluation of the proposed control system encompasses various scenarios, accounting for system parameter fluctuations and load disturbances:

Scenario 1: Nominal system parameters
Scenario 2: 35% increase in system parameters
Scenario 3: 35% decrease in system parameters

4.4.1 Scenario 1: Nominal Parameters

Simulation results for Scenario 1 are depicted in Figures 3 - 8. These figures portray frequency deviation, ΔPtie signal power deviation (left graph), and control error in distinct zones (right graph).

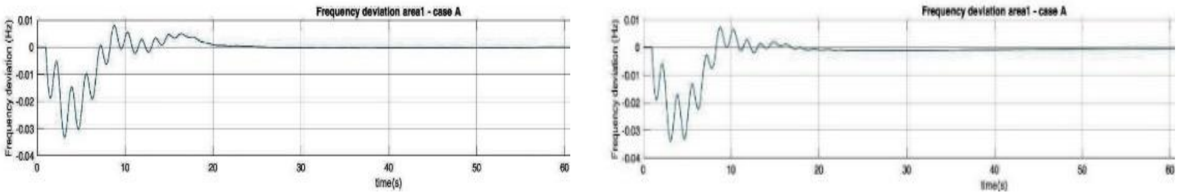

Figure 3. Scenario 1 for Region 1: Different parameters simulation results.

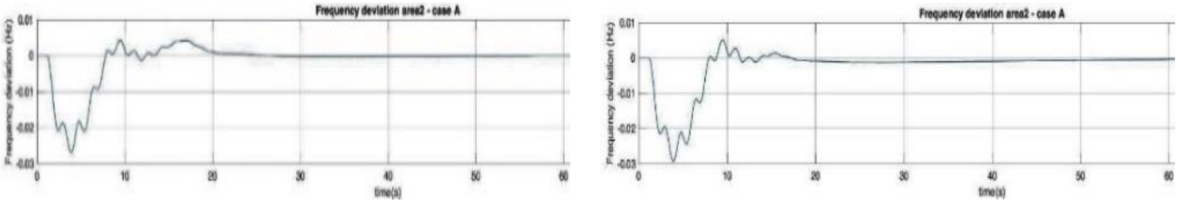

Figure 4. Scenario 1 for Region 2: Constant and varying parameters.

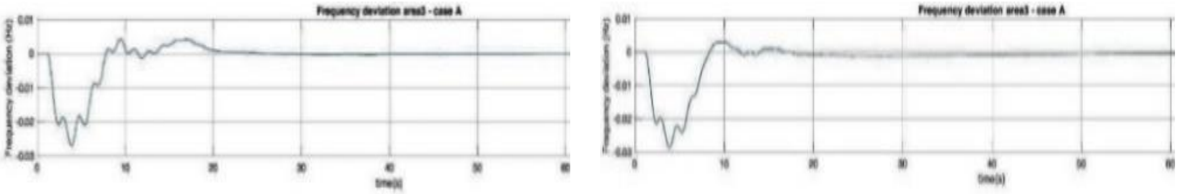

Figure 5. Scenario 1 for Region 3: Constant and varying parameters.

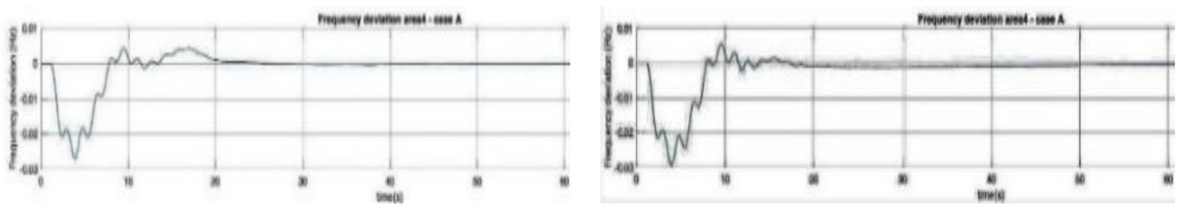

Figure 6. Scenario 1 in Region 4: Constant and Varying Parameters

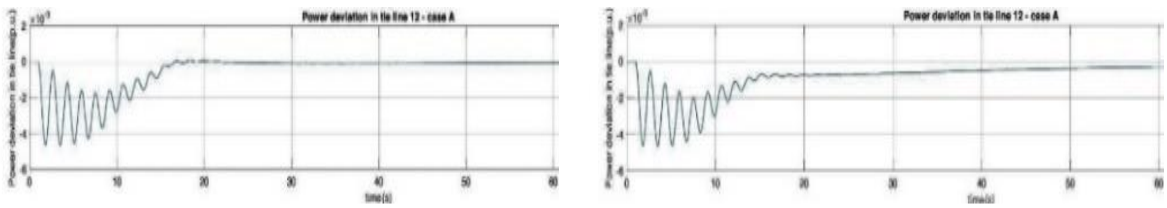

Figure 7. Power Spectral Density of Communication Signal in Scenario 1 Across Four Regions

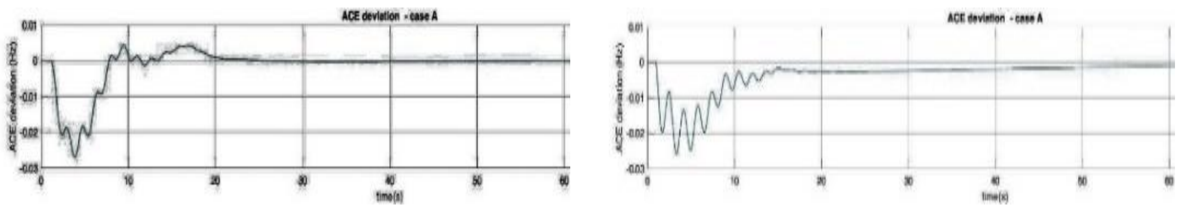

Figure 8. Scenario 1: Control Error Across Four Regions

Performance metrics (Settling Time, Peak Undershoot, ISE) are summarized in Tables 4, 5,6 and 7 for the proposed controller with constant and varying parameters.

Table 4. Scenario 1 Step Response with 5% Bandwidth: Fixed vs. Variable Parameters

Controllers	**Δf_1**	**Δf_2**	**Δf_2**	**Δf_4**	**ΔP_{tie}**	**E_I**
Constant parameters	17.7355	17.7230	17.7230	17.7230	13.1227	11.6211
Different parameters	17.0599	17.3420	17.3420	17.3897	13.4724	13.1036

Table 5. Peak Undershoot Performance of Scenario 1 Controller: Constant vs. Varying Parameters

Controllers	Δf_1	Δf_2	Δf_2	Δf_4	ΔP_{tie}	E_I
Constant parameters	-0.0250	-0.0046	-0.0273	-0.0273	-0.0273	-0.0325
Different parameters	-0.0205	-0.0046	-0.0289	-0.0293	-0.0295	-0.0338

Table 6. Frequency Deviation Error Dynamics: Fixed vs. Variable Parameters

Controllers	Δf_1	Δf_2	Δf_2	Δf_4	ΔP_{tie}	E_I
Constant parameters	0.0661	0.0148	0.0659	0.0659	0.0659	0.0745
Different parameters	0.0855	0.0210	0.0689	0.0689	0.0695	0.0774

4.4.2 Scenario 2: System Parameter Sensitivity

This section assesses controller stability amid changing system parameters. Simulations involve a 1% load disturbance in Region 1, where key parameters such as B_i, T_i, J, and Tp_i increase by 35%. Results provide insights into controller adaptability in dynamic conditions. Simulation results for all controllers are depicted in Figures 9-11, showcasing responses in frequency, tie-line power, and control error. These figures offer a detailed visual representation of the system's behaviour with the proposed controller, facilitating a nuanced comprehension of its performance.

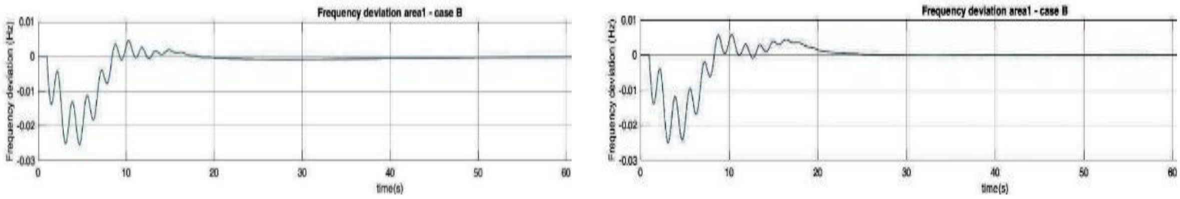

Figure 9. Scenario 2 Parameter Sequencing Across Regions (Region 1)

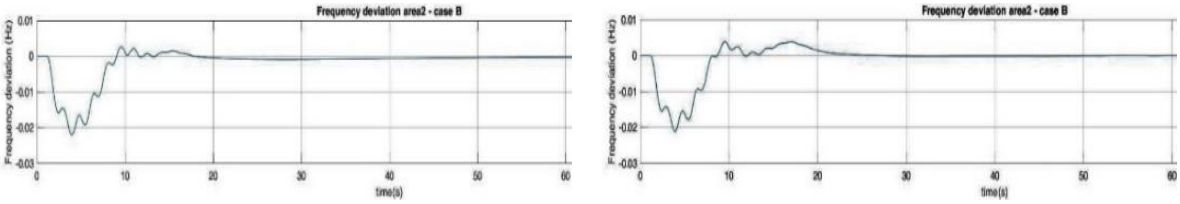

Figure 10. Scenario 2 Parameter Sequencing Across Regions (Region 2)

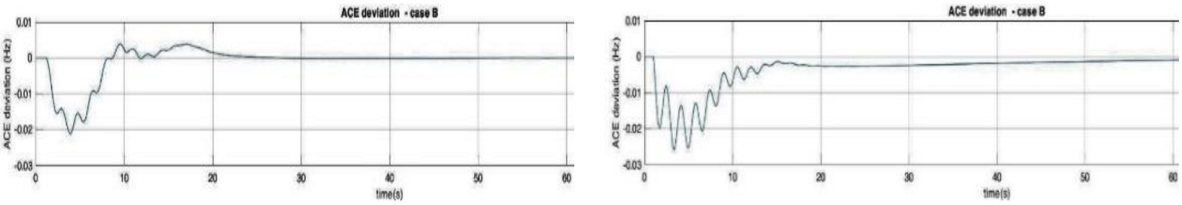

Figure 11. Control Error Signal for Scenario 2 Across Four Regions with Varied Parameters

Furthermore, performance quantification is facilitated through the following key metrics:

Table 7. Scenario 2 Controller Dynamics: Constant vs. Varied Parameters (5%Bandwidth)

Controllers	Δf_1	Δf_2	Δf_2	Δf_4	ΔP_{tie}	ACE_I
Constant parameters	11.5768	13.2041	18.3002	18.3002	18.3002	18.3836
Different parameters	13.0283	13.4435	17.7740	17.7104	17.8262	18.0433

Table 8. Peak Undershoot for Scenario 2: Constant vs. Varied Parameters

Controllers	Δf_1	Δf_2	Δf_2	Δf_4	ΔP_{tie}	ACE_I
Constant parameters	-0.0253	-0.0046	-0.0211	-0.0211	-0.0211	-0.0245
Different parameters	-0.0257	-0.0046	-0.0220	-0.0222	-0.0225	-0.0261

Table 9. Frequency Deviation Error Dynamics for Scenario 2: Constant vs. Varied Parameters

Controllers	**Δf_1**	**Δf_2**	**Δf_2**	**Δf_4**	**ΔP_{tie}**	**ACE_1**
Constant parameters	0.0706	0.0149	0.0579	0.0579	0.0579	0.0650
Different parameters	0.0826	0.0206	0.0540	0.0542	0.0541	0.0598

4.4.3 Scenario 3: Parameter Variation

To assess controller performance, we tested another system subjected to a 1% load disturbance in region 1. The system parameters (B_i, T_i, J, Tp_i), optimized by the intelligent fuzzy PID controller, remained unchanged while reduced by 35% from nominal values. Simulation results and analyses for this scenario are presented in Figures 12-17.

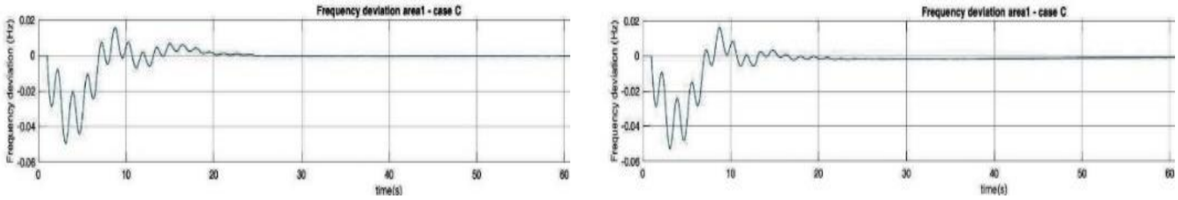

Figure 12. Scenario 3 Parameter Order Across Four Regions (Region 1): Constant vs. Varied Parameters

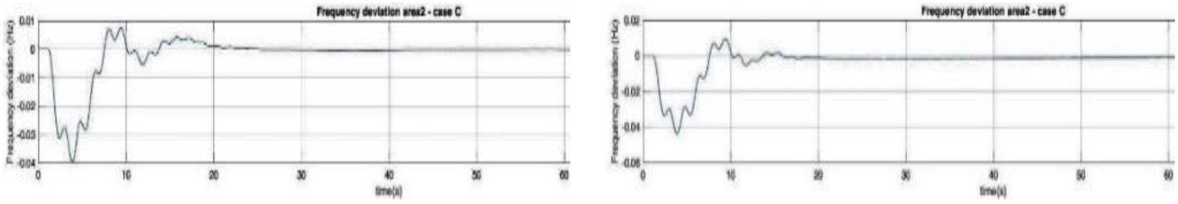

Figure 13. Scenario 3 (Region 2) constant and different parameters in four regions

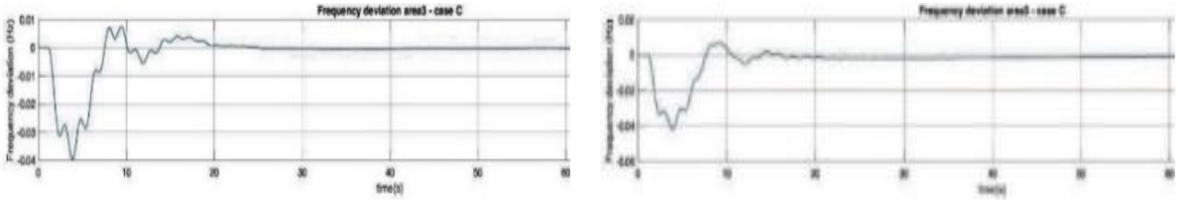

Figure 14. Scenario 3 (Region 2) constant and different parameters in four regions

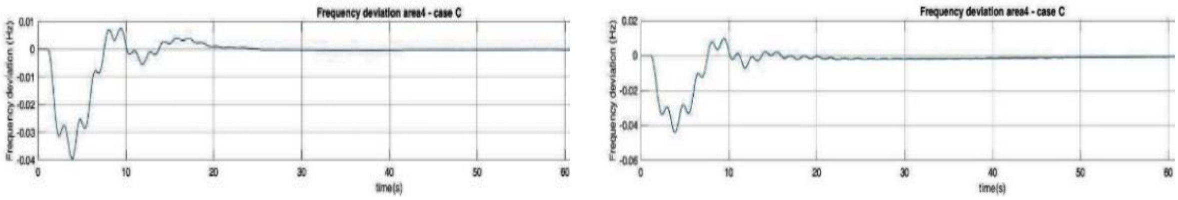

Figure 15. Scenario 3 Parameter Comparison Across Zones (Zone 4): Constant vs. Varied Parameters

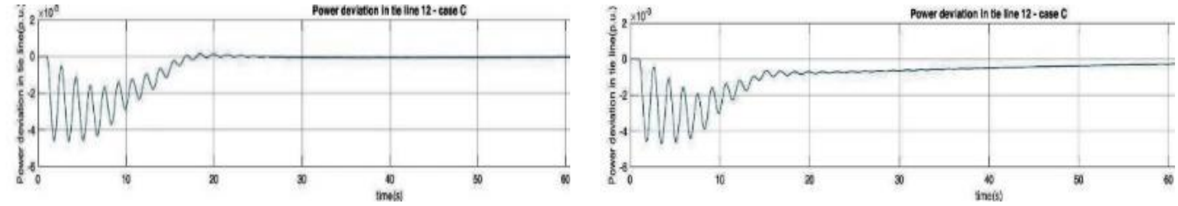

Figure 16. Communication Power Signal in Scenario 3 Across Four Regions: Constant vs. Varied Parameters

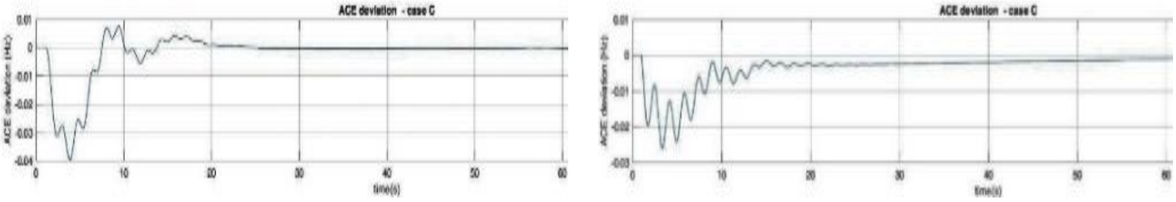

Figure 17. Control Error Signal in Scenario 3 Across Four Regions: Constant vs. Varied Parameters

Performance metrics for this comparison are summarized in Tables 10-12.

Table 10. Settling Time Dynamics for Scenario 3 (5% Bandwidth) Across Four Regions

Controllers	**Δf_1**	**Δf_2**	**Δf_2**	**Δf_4**	**ΔPtie**	**ACE_1**
Constant parameters	13.9871	13.7849	16.2843	16.1875	16.1685	16.1578
Different parameters	13.2254	13.4495	16.3897	16.2148	16.4944	16.7134

Table 11. Peak Undershoot Dynamics for Scenario 3 Across Four Regions

Controllers	**Δf_1**	**Δf_2**	**Δf_2**	**Δf_4**	**ΔPtie**	**ACE_1**
Constant parameters	-0.0236	-0.0041	-0.0465	-0.0497	-0.0489	-0.0589
Different parameters	-0.0251	-0.0046	-0.0422	-0.0434	-0.0427	-0.0507

Table 12. Dynamic Frequency Deviation Error Performance for Scenario 3 (5% Bandwidth) Across Four Regions

Controllers	**Δf_1**	**Δf_2**	**Δf_2**	**Δf_4**	**ΔPtie**	**ACE_1**
Constant parameters	0.0896	0.0257	0.0984	0.9984	0.0964	0.1106
Different parameters	0.0851	0.0210	0.0995	0.1001	0.0987	0.1117

4.5 Frequency Deviation Response and Validation

Figures 18-21 present the frequency deviation response of the proposed controller across various conditions with varying parameter values. These figures underscore the minimal impact of operational and system parameter fluctuations on frequency deviation, confirming the controller's stability.

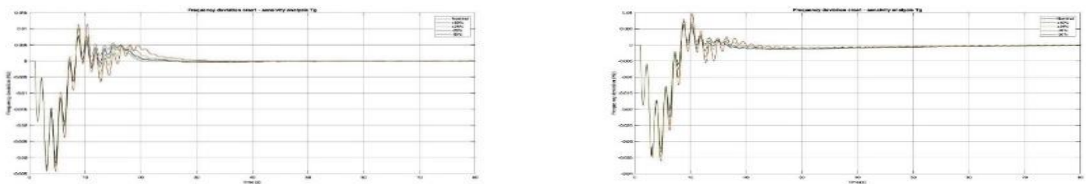
Figure 18. Frequency Deviation in Region 1 (T_g Parameter): Constant vs. Varied Parameters


Figure 19. Frequency Deviation in Region 1 (T_t Parameter): Constant vs. Varied Parameters

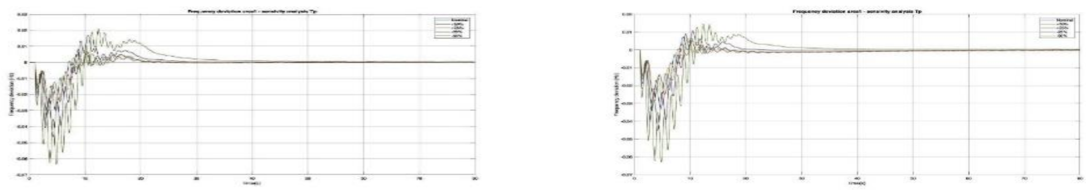
Figure 20. Frequency Deviation in Region 1 (T_p Parameter): Constant vs. Varied Parameters

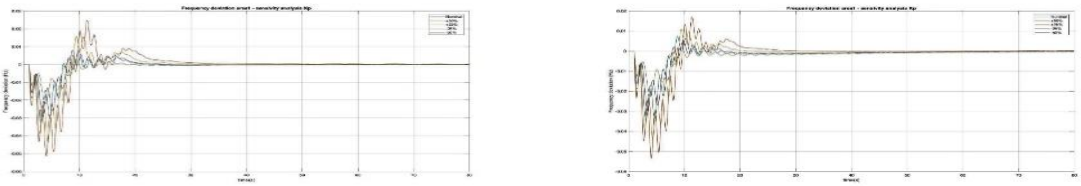

Figure 21. Frequency Deviation in Region 1 (K_p Parameter): Constant vs. Varied Parameters

The figures confirm the proposed controller's stability under various load conditions, swiftly bringing deviations to target values without needing extensive parameter adjustments. A random load disturbance was introduced in region 1 at t = 2 seconds which helps explore and validate the controller's effectiveness, with Figures 22 and 23 illustrate the accurate coding and controller behaviour.

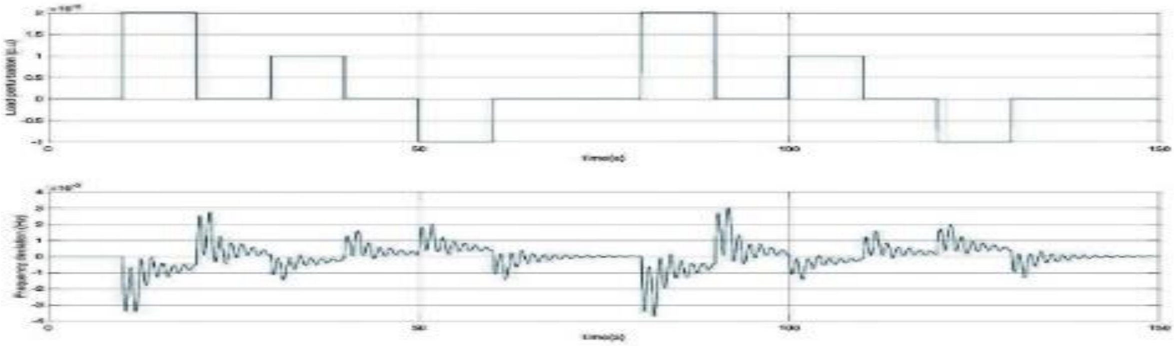

Figure 22. Frequency deviation of the load loading based on the coding state.

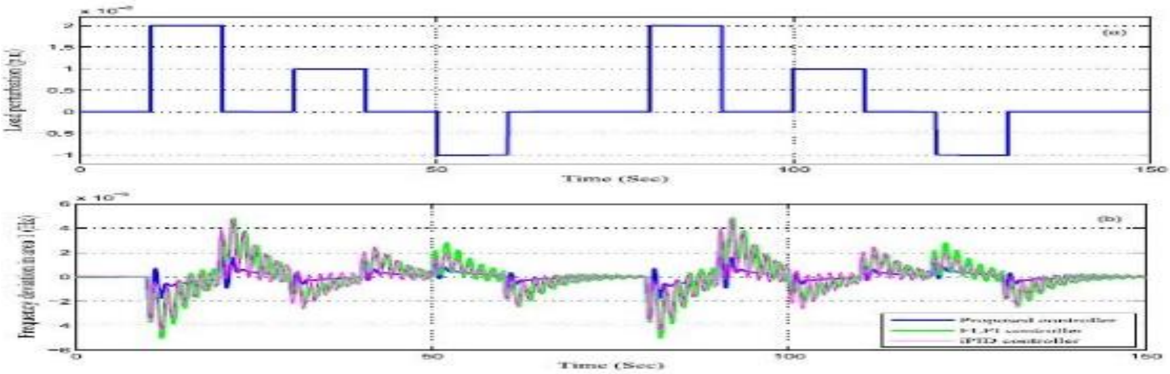

Figure 23. Frequency deviation of the load loading based on the actual state.

5 DISCUSSION AND CONCLUSION

ACO and PSO exhibit distinct convergence patterns and results, with ACO showing steady convergence over generations and PSO converging more rapidly over iterations. The choice between the techniques depends on the desired balance between exploration and exploitation. The optimized parameters from both ACO and PSO were applied to the fuzzy PID controller model, providing insights into their effectiveness in optimizing the intelligent fuzzy-hybrid PID controller for Load Frequency Control in power systems. The simulations validate the efficacy of the fuzzy PID controller optimized by PSO, ensuring stable load frequency control under various conditions. PSO demonstrates faster convergence and superior optimization compared to GA and ACO. However, further research on hybrid GA-PSO approaches is recommended to leverage the strengths of both algorithms.

In conclusion, the proposed intelligent fuzzy control strategy enables robust frequency regulation and disturbance rejection, demonstrating its potential for practical application.

REFERENCES

Abdelaziz, A.Y., Mekhamer, S.F. and Al-Kharashi, M.L. (2016). Adaptive PID controller based on particle swarm optimization and neural network for power system stability. *International Journal of Electrical Power & Energy Systems, vol. 83*, pp. 67-76.

Abdel-Magid, Y. and Dawoud, M. (1995). *Genetic algorithms applications in load frequency control*.

Afzalan, A. and Jurabian, M. (2014). Frequency Load Controller Design for Interconnected Power Systems using Search Optimization Algorithm (SOA). *Computational Intelligence in Electrical Engineering (Intelligent Systems in Electrical Engineering), vol. 5*, no. 2, pp. 1393.

Çam, E. and Kocaarslan, İ. (2005). Load Frequency Control in Two Area Power Systems Using Fuzzy Logic Controller. *Energy Conversion and Management, vol. 46*, pp. 233-243, 01/31.

Delassi, A., Arif, S. and Mokrani, L. (2018). Load frequency control problem in interconnected power systems using robust fractional pi λ D controller. *Ain Shams Engineering Journal, vol. 9*(1), pp. 77–88. doi:10.1016/j.asej.2015.10.004.

Dhillon, S. S., Lather, J. S. and Marwaha, S. (2015). Multi Area Load Frequency Control Using Particle Swarm Optimization and Fuzzy Rules. *Procedia Computer Science, vol. 57*, pp. 460-472.

Dhillon, S. S., Lather, J. S. and Marwaha, S. (2016). Multi objective load frequency control using hybrid bacterial foraging and particle swarm optimized PI controller. *International Journal of Electrical Power & Energy Systems, vol. 79*, pp. 196-209.

Dong, L., Zhang, Y. and Gao, Z. (2012). A robust decentralized load frequency controller for interconnected power systems. *ISA Transactions, vol. 51*, no. 3, pp. 410-419.

El-Bahay, M., Lotfy, M. and Abd El-Hameed, M. (2022). Computational Methods to Mitigate the Effect of High Penetration of Renewable Energy Sources on Power System Frequency Regulation: A Comprehensive Review. *Archives of Computational Methods in Engineering*. *vol. 30*. doi:10.1007/s11831-022-09813-9.

Haroun, A. G., and Li, Y.-Y. (2017). A novel optimized hybrid fuzzy logic intelligent PID controller for an interconnected multi-area power system with physical constraints and boiler dynamics. *ISA transactions, vol. 71*, pp. 364-379.

Haroun, A. G., and Li, Y.-Y. (2019). Ant Lion Optimized Fractional Order Fuzzy Pre-Compensated Intelligent Pid Controller for Frequency Stabilization of Interconnected Multi-Area Power Systems. *Applied System Innovation*, *vol. 2*, no. 2.

Kennedy, J. and Eberhart, R.C. (1995). Particle swarm optimization. *Proceedings of ICNN'95-International Conference on Neural Networks, vol. 4*, pp. 1942-1948.

Li, X., Wang, Y., Li, N., Han, M., Tang, Y. and Liu, F. (2017). Optimal fractional order PID controller design for automatic voltage regulator system based on reference model using particle swarm optimization. *International Journal of Machine Learning and Cybernetics. vol 8*, pp. 1595–1605. doi: 10.1007/s13042-016-0530-2Meena, A. R. and Kumar, S. S. (2016). Genetically tuned fuzzy PID controller in two area reheat thermal power system. *Russian Electrical Engineering, vol. 87*, no. 10, pp. 579-587.

Monfared, S. B., Ebrahimi, A. and Parsa, A. (2017). Design of Robust H_∞ Control for Stabilizing of Stratospheric Airship with Parametric Uncertainty and External Disturbance. *Modares Mechanical Engineering, vol. 17*, no. 3, pp. 216-226.

Panda, G., Panda, S. and Ardil, C. (2009) Automatic Generation Control of Interconnected Power System with Generation Rate Constraints by Hybrid Neuro Fuzzy Approach. *World Academy of Science, Engineering and Technology*, pp. 543-548.

Pandey, S., Dwivedi, P. and Junghare, A. S. (2017). A novel 2-DOF fractional-order PI λ - D μ controller with inherent anti-windup capability for a magnetic levitation system. *AEU - International Journal of Electronics and Communications, vol. 79*, 05/01.

Saadat, H. (1999). *Power System Analysis*. WCB/McGraw-Hill.

Sadaqati, R., Shahidi, F. A., & Mazarei, M. (2016). Improved Frequency Control of Microgrid Load Islands Using Fuzzy Controller. *1st International Conference on Innovative Research Achievements in Electrical and Computer Engineering, Tehran.*

Sahu, R. K., Panda, S. and Sekhar, G. C. (2015). A novel hybrid PSO-PS optimized fuzzy PI controller for AGC in multi area interconnected power systems. *International Journal of Electrical Power & Energy Systems, vol. 64*, pp. 880-893.

Sahu, R. K., Panda, S. and Yegireddy, N. K. (2014). A novel hybrid DEPS optimized fuzzy PI/PID controller for load frequency control of multi-area interconnected power systems. *Journal of Process Control, vol. 24*, no. 10, pp. 1596-1608.

Shayeghi, H. and Shayanfar, H. A., (2006). Application of ANN technique based on μ-synthesis to load frequency control of interconnected power system. *International Journal of Electrical Power & Energy Systems, vol. 28*

Singh, V. P., Mohanty, S.R., Kishor, N. and Ray, P. K. (2013). Robust H-infinity load frequency control in hybrid distributed generation system. International *Journal of Electrical Power & Energy Systems, vol. 46*, pp.294-305.

Talaq, J. and Al-Basri, F. (1999). Adaptive fuzzy gain scheduling for load frequency control. *IEEE Transactions on Power Systems, vol. 14*(1), pp. 145–150. doi:10.1109/59.744505.

Tripathy, S., Hope, G. and Malik, O. (1982). Optimisation of load-frequency control parameters for power systems with reheat steam turbines and governor deadband nonlinearity. IEE Proceedings C (Generation, Transmission and Distribution), vol. 129, no. 1, pp. 10-16.

Vasant, P., Barsoum, N. and Webb, J. (2011). *Innovation in Power, Control, and Optimization: Emerging Energy Technologies*. IGI Global.

Vrabie, D., Pastravanu, O., Abu-Khalaf, M. and Lewis, F. L. (2009). Adaptive optimal control for continuous-time linear systems based on policy iteration. *Automatica, vol. 45*, pp.477-484.

Wenhui, Z., & Ye, X., Jiang, L. and Yamin, F. (2014). Robust Control for Robotic Manipulators Base on Adaptive Neural Network. *The Open Mechanical Engineering Journal*, *vol. 8*. pp. 497-502. doi:10.2174/1874155X01408010497

Zhang, H., Chen, D., Xu, B.-B. and Wang, F. (2015). Nonlinear modelling and dynamic analysis of hydro-turbine governing system in the process of load rejection transient. *Energy Conversion and Management, vol. 90*, pp. 128-137, 01/15.